THE JOURNAL OF BIOLOGICAL CHEMISTRY VOL. 284, NO. 49, pp. 33781–33788, December 4, 2009

MAPK Pathway Activation Delays G_2/M Progression by Destabilizing Cdc25B*[S]

Received for publication, May 29, 2009, and in revised form, September 30, 2009 Published, JBC Papers in Press, October 1, 2009, DOI 10.1074/jbc.M109.027516

Puji Astuti[‡1], Tanya Pike[‡1], Charlotte Widberg[‡], Elizabeth Payne[‡], Angus Harding[§], John Hancock[¶2,3], and Brian Gabrielli[‡2,4]

From the [‡]Diamantina Institute for Cancer Immunology and Metabolic Medicine, [§]Queensland Brain Institute, and [¶]Institute of Molecular Biosciences, University of Queensland, Brisbane 4102, Queensland, Australia

Activation of the mitogen-activated protein kinase (MAPK) pathway by growth factors or phorbol esters during G_2 phase delays entry into mitosis; however, the role of the MAPK pathway during G_2/M progression remains controversial. Here, we demonstrate that activation of the MAPK pathway with either epidermal growth factor or 12-*O*-tetradecanoylphorbol-13-acetate induces a G_2 phase delay independent of known G_2 phase checkpoint pathways but was specifically dependent on MAPK/extracellular signal-regulated kinase kinase (MEK1). Activation of MAPK signaling also blocked exit from a G_2 phase checkpoint arrest. Both the G_2 phase delay and blocked exit from the G_2 checkpoint arrest were mediated by the MEK1-dependent destabilization of the critical G_2/M regulator cdc25B. Reintroduction of cdc25B overcame the MEK1-dependent G_2 phase delay. Thus, we have demonstrated a new function for MEK1 that controls G_2/M progression by regulating the stability of cdc25B. This represents a novel mechanism by which factors that activate MAPK signaling can influence the timing of entry into mitosis, particularly exit from a G_2 phase checkpoint arrest.

The canonical MAPK[5] pathway of Ras, Raf, MEK, and ERK provides a sensitive mechanism for transducing extracellular signals critical for cell growth and development (1). ERK-dependent phosphorylation of a broad range of substrates is the primary signaling output of the pathway (2). The ability of the MAPK pathway to influence entry into the cell cycle has been well established (3–5). Signaling through this pathway also has a role in G_2 phase (6–8), possibly to regulate Golgi disassembly (9).

Growth factors activate the canonical MAPK pathway through specific receptors, whereas the tumor-promoting phorbol esters activate this pathway via PKC (10). When either growth factors or phorbol esters are added in G_2 phase they can induce a G_2 phase cell cycle delay (11, 12); however, the exact mechanism of the delay is poorly understood. Activation of the MAPK pathway by growth factors and phorbol esters has been implicated in the G_2 phase delay (13), with the ERK-dependent up-regulation of the cdk inhibitor $p21^{WAF1}$ identified as a key component of the delay (13). Other mechanisms, including increased protein phosphatase 2A activity, have also been proposed (14).

Cells respond to a variety of stresses by imposing a G_2 phase delay through the action of cell cycle checkpoint mechanisms. The checkpoint mechanisms impose the arrest by blocking activation of cyclin B/cdk1, the driver of mitosis. Major checkpoint mechanisms demonstrated to impose a G_2 phase arrest in response to DNA damage are the ATM and related ATR-dependent pathways. ATM and ATR are the apical components of pathways that signal through Chk1 and Chk2 to block cdc25-dependent activation of the mitotic cyclin/cdks (15). The p38MAPK-MAPKAPK2 pathway is involved in a separate G_2 arrest pathway (16, 17).

These pathways all target the key G_2/M transitional regulators, the cdc25 family of dual specificity phosphatases. The cdc25s activate the mitotic cdk complexes by dephosphorylating the inhibitory Thr^{14} and Tyr^{15} residues on cdk1 and cdk2. All three cdc25 isoforms appear to have roles in G_2/M progression, although only depletion of cdc25A and cdc25B delays entry into mitosis (18). Both cdc25A and cdc25B are unstable proteins, and their activity is in part regulated by their stability, which is increased in G_2/M and decreased in response to stresses (19–21). All three cdc25 isoforms are targets for checkpoint kinase inactivation (22). Cdc25A is destabilized by Chk1 phosphorylation in response to DNA damage (23). Cdc25B is specifically required for exit from the G_2 phase checkpoint arrest (24), and its stability has also been linked to responses to damage (25). The possibility that MAPK signaling induces a G_2 delay via the ATM/ATR, Chk1/2, or p38MAPK checkpoint pathways has not been reported. Here, we demonstrate that the MAPK signaling-induced G_2 phase delay is independent of usual G_2 checkpoint mechanisms, but instead is a consequence of MEK1-dependent destabilization of the critical G_2/M regulator cdc25B.

EXPERIMENTAL PROCEDURES

Materials—Etoposide, caffeine, ICRF193, epidermal growth factor (EGF), and 12-*O*-tetradecanoylphorbol-13-acetate (TPA)

* This work was supported by grants from the Australian Research Council.
[S] The on-line version of this article (available at http://www.jbc.org) contains supplemental Figs. S1–S5.
[1] Both authors contributed equally to this work.
[2] National Health and Medical Research Council Senior Research Fellow.
[3] Present address: Dept. of Integrative Biology and Pharmacology, University of Texas Health Science Center, Houston, TX 77030.
[4] To whom correspondence should be addressed: Diamantina Institute for Cancer Immunology and Metabolic Medicine, University of Queensland, Princess Alexandra Hospital, Brisbane, Queensland 4102, Australia. Fax: 61-7-3240-5946; E-mail: brianG@uq.edu.au.
[5] The abbreviations used are: MAPK, mitogen-activated protein kinase; cdk, cyclin-dependent kinase; EGF, epidermal growth factor; ERK, extracellular signal-regulated kinase; GFP, green fluorescent protein; MEF, mouse embryonic fibroblast; MEK, MAPK/ERK kinase; PKC, protein kinase C; siRNA, small interfering RNA; TPA, 12-*O*-tetradecanoylphorbol-13-acetate; ATM, ataxia telangiectasia mutated; ATR, ATM-Rad3 related.

were purchased from Sigma-Aldrich. The MEK1/2 inhibitor U0126 was purchased from Cell Signaling Technology, and the PKC inhibitor Gö6976 was from Calbiochem. Antibodies to MEK1, MEK2, ERK2, cdc25A, and cdc25B were obtained from Santa Cruz Biotechnology. Phospho-p44/42 (phospho-ERK), phospho-MEK1/2 $Ser^{218/222}$, phospho-MEK1 Thr^{286}, cdk1 $Tyr(P)^{15}$, γH2AX, and Chk2 were obtained from Cell Signaling Technology. $p21^{CIP1}$ was from Calbiochem. α-Tubulin antibody was from Sigma-Aldrich. Chk1 and MEK1 (clone Y77) were from Abcam. Cdc25C and cyclin B1 antibodies were as described previously (19).

Cell Lines and Culture Conditions—HeLa cells were maintained in Dulbecco's modified Eagle's medium and supplemented with 5% donor bovine serum (Serum Supreme; BioWhittaker, Inc.), 20 mM HEPES (Sigma), 25 mM sodium pyruvate (Invitrogen), and 2 mM L-glutamine (Invitrogen). U2OS osteosarcoma cells and tetracycline-inducible cdc25B U2OS cells (26) were maintained in 10% fetal bovine serum containing medium with 2 μg/ml tetracycline to suppress cdc25B expression. All cell lines were maintained in a 5% CO_2-humidified incubator at 37 °C. HeLa cells were arrested with 1 μM etoposide for 16 h and then released to enter mitosis with 5 mM caffeine. U2OS cells were treated with 2 μM ICRF193 for 16 h. Where required, 20 μM U0126, 0.1 μM TPA, 100 ng/ml, or 1 μg/ml EGF was added to cultures a half-hour before caffeine addition. HeLa cells were synchronized using thymidine, and U2OS cells were synchronized with overnight treatment with 2 mM hydroxyurea as described previously (19). Where required, Gö6976, U0126 and/or TPA, and EGF were added at 7 h after the synchrony release.

siRNA Transfections—HeLa cells were transfected with siRNAs against the following sequences: MEK1, 5′-aagcaactcatggttcatgcttt-3′; MEK1.2, 5′-aaccagcccagcacaccaacc-3′; MEK2, 5′-aagaaggagagcctcacagca-3′; Chk1, 5′-aactgaagaagcagtcgcagt-3′; Chk2, 5′-aaacgccgtcctttgaatatt-3′. p21 knockdown was achieved using Dharmacon ON-TARGETplus SMARTpool siRNA targeted to p21. For MEK and p21 knockdown experiments, the scrambled siRNA sequence 5′-aatgatctacctgttaagagtcctgtctc-3′ was used as a control, whereas for the Chk1 and Chk2 knockdown experiments the nontargeting control siRNA (5′-aatagcgactaaacacatcaacc-3′) was used. With the exception of the p21 siRNA from Dharmacon, all siRNA constructs were made using the Ambion siRNA construction kit (Ambion, Inc., Austin TX) according to the manufacturer's instructions. Transfections were carried out in 6- or 12-well plates using Lipofectamine 2000 (Invitrogen) according to the manufacturer's instructions. For effective MEK1 and MEK2 knockdown, 40 nM siRNA was used per well. In Chk1 experiments, a 20 nM concentration of each siRNA construct was pooled and transfected per well, and 50 nM Chk2 siRNA per well was used. The medium was replaced with fresh complete medium 4 h after transfection, and cells were left for 24 h, or 48 h in the case of Chk2 knockdown.

Immunoblotting—Cells were lysed in NETN buffer (100 mM NaCl, 1 mM EDTA, 0.5% Nonidet P-40, 20 mM Tris, pH 8) supplemented with 5 μg/ml aprotinin, 5 μg/ml pepstatin, 5 μg/ml leupeptin, 0.5 mM phenylmethylsulfonyl fluoride, 30 mM NaF, 0.1 mM sodium orthovanadate, 25 mM β-glycerophosphate, and 0.1% SDS. Protein quantification of the cleared lysates was carried out using Bio-Rad protein assay reagent with bovine serum albumin as a standard. Samples (20 μg of protein) were resolved on 10 or 12% SDS-PAGE and then transferred to nitrocellulose membranes (Amersham Biosciences) via a semidry transfer system (Bio-Rad). Proteins were probed with the indicated antibodies, followed by horseradish peroxidase-conjugated secondary antibodies (Zymed Laboratories Inc.) and detected by enhanced chemiluminescence.

Mutagenesis of Cdc25B Ser^{249} to Ala—PCR site-directed mutagenesis was performed according to the manufacturer's protocol. Mutagenic primer 5′-GGAAGATGGAAGTGGAGGAGCTCGCACCCCTGGCCCTA-3′ was used to convert Ser^{249} to Ala in pEGFP-cdc25B3. The half-life of cdc25B was examined by overexpressing the wild-type and the mutant GFP-cdc25B in HeLa cells, which were then synchronized with thymidine overnight. Cycloheximide (10 μg/ml) was added 6 h after transfection in the presence or absence of TPA and harvested at the indicated time points. The lysates were immunoblotted for GFP-cdc25B using GFP antibody (Roche Applied Science).

Immunoprecipitation—HeLa cells were synchronized using double thymidine synchrony, and drugs were added 7 h after release for 30 min. The cells were lysed in NETN buffer. For immunoprecipitation of cdc25B from cell lysates, cell lysates were precleared with 50 μl of 50% protein A-Sepharose beads (Amersham Biosciences) and incubated with primary antibody overnight at 4 °C, and then immunue complexes were precipitated with protein A-Sepharose slurry for 2 h. Cdc25B immunoprecipitates were probed for $Ser(P)^{249}$-cdc25B in the presence of nonphosphorylated peptide (kindly provided by Prof. Ducommun) and cdc25B (Santa Cruz Biotechnology).

Live Cell Time Lapse Microscopy—Time lapse movies were produced using a Zeiss Axiovert 200M cell observer with 37 °C incubator hood and 5% CO_2 cover. Digital images were taken every 10–15 min with a Zeiss AxioCam, and the images were processed using AxioVision software. Cumulative mitotic cell counts were performed by following cells in four or five random fields over several hours. The time at which cells entered mitosis was recorded for each cell in the field. The fields were combined and reported as a percentage of the total number of cells in the field at the start of the experiments. The data presented are typical of at least three independent experiments.

RESULTS

MAPK Pathway-induced G_2 Delay Is Dependent on Destabilization of Cdc25B—To examine the G_2 phase delay imposed by activation of MAPK signaling, synchronized HeLa cells were treated with and without TPA in early G_2 phase, 7 h after release from synchrony arrest. Following the cells with time lapse microscopy revealed that the addition of TPA delayed entry into mitosis by 2–3 h and that inhibiting the MEK activity with 20 μM UO126, sufficient to block ERK activation completely (data not shown), reduced the delay (Fig. 1*A*). Immunoblotting similar samples for phospho-MEK1 Thr^{286}, a cyclin B/cdk1 substrate (27) and marker of mitosis (28), confirmed the delayed entry into mitosis with the addition of TPA. Analysis of cyclin B1/cdk1 revealed that TPA addition blocked the dephos-

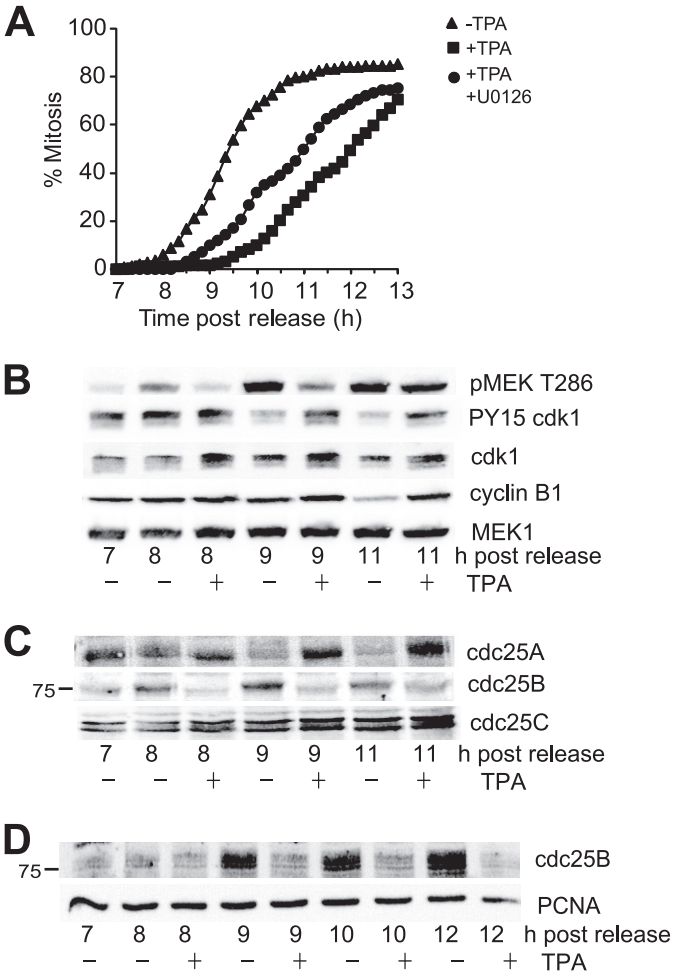

FIGURE 1. **TPA-induced G_2 phase delay correlated with destabilization of cdc25B.** *A*, synchronized HeLa cells were treated with (*squares*) or without TPA (*triangles*) in early G_2 phase (7 h after synchrony release) or with TPA and UO126 (*circles*) followed by time lapse microscopy, and the cumulative mitotic index was assessed. *B*, cells from a similar experiment were immunoblotted for phospho-MEK1 Thr^{286} (*pMEK T286*) as a marker of cyclin B/cdk1 activity and mitosis, the inactive Tyr^{15}-phosphorylated cdk1 (*PY15 cdk1*), cdk1, cyclin B1, and MEK1. *C*, the same lysates as in *B* were immunoblotted for the three cdc25 isoforms. The position of the 75 kDa marker is shown on the cdc25B blot. *D*, U2OS cells were synchronized, and 7 h after release from the synchrony arrest (G_2 phase), TPA was added, and cells were harvested at the indicated times. Lysates were immunoblotted for cdc25B. Proliferating cell nuclear antigen (*PCNA*) is a loading control.

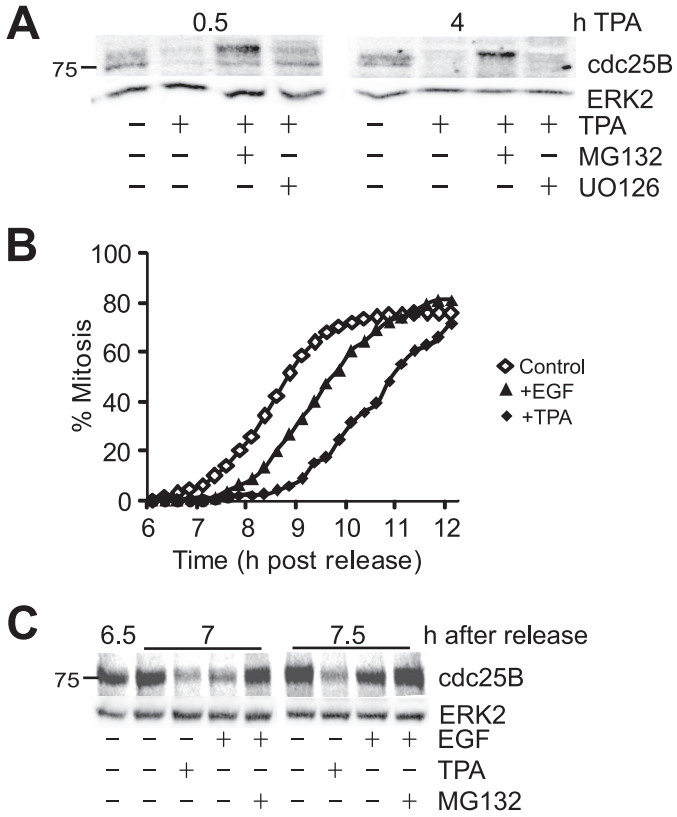

FIGURE 2. **TPA and EGF induce destabilization of cdc25B.** *A*, G_2 phase HeLa cells were treated with or without TPA, the proteasome inhibitor MG132, and U0126, harvested 0.5 and 4 h after TPA treatment, and immunoblotted for cdc25B. ERK2 was immunoblotted as a loading control. *B*, thymidine-synchronized HeLa cells were treated with either 100 ng/ml EGF (*triangles*), TPA (*solid diamonds*) or untreated (*open diamonds*) followed by time lapse microscopy, and the cumulative mitotic index was assessed. *C*, cells from an experiment similar to *B* were treated with the indicated drugs at 6.5 h after synchrony release, harvested at 7 and 7.5 h, then immunoblotted for cdc25B and ERK2 protein as a loading control.

phorylation of Tyr^{15} on cdk1, thereby blocking activation of cyclin B1/cdk1 (Fig. 1*B*).

The block in cyclin B/cdk1 activation suggested that TPA affected cdc25 function. Immunoblotting for the three cdc25 isoforms revealed that TPA had opposite effects on cdc25A and cdc25B and no effect on cdc25C (Fig. 1*C*). TPA appeared to stabilize cdc25A levels; however, this was simply a block in the destruction of cdc25A that occurs during the transit through mitosis (Fig. 1*C*; cdc25A peaks at 8 h and is significantly reduced by 9 h, correlated with maximal phospho-MEK Thr^{286} levels in the controls). These results show that cdc25A levels are not regulated by the addition of TPA and therefore are unlikely to be important in the TPA-mediated G_2 delay. Cdc25B levels increased during progression into mitosis in the controls, but in contrast to cdc25A, TPA treatment completely blocked cdc25B increase (Fig. 1*C*). The loss of cdc25B was also observed in synchronized U2OS cells treated with TPA in early G_2 phase (Fig. 1*D*). Addition of the proteasome inhibitor MG132 completely blocked the loss of cdc25B, confirming that the loss of cdc25B after the TPA addition was through destabilization of the cdc25B protein (Fig. 2*A*). Interestingly, the addition of UO126 only partly rescued the destabilization of cdc25B (Fig. 2*A*), which may explain the inability of UO126 to rescue the TPA induced delay completely (Fig. 1*A*).

Activation of MAPK signaling by EGF also induced a G_2 phase delay and rapid destabilization of cdc25B, although the effect was not as robust as observed with TPA. Addition of 100 ng/ml EGF to early G_2 phase cells delayed entry into mitosis by at least 1 h (Fig. 2*B*). Addition of EGF also promoted the rapid destabilization of cdc25B to an extent similar to that of TPA, within 30 min of the EGF addition (7 h after release). The effect was not as long lived as TPA, with cdc25B levels increasing by 7.5 h and completely recovered by 8 h (Fig. 2*C* and data not shown). Importantly, inhibition of proteasome activity by MG132 completely blocked the EGF-induced loss of cdc25B levels.

MAPK Activation Blocks Exit from G_2 Checkpoint Arrest by Destabilizing Cdc25B—Cdc25B is specifically required for exit from a DNA damage G_2 phase checkpoint arrest triggered by

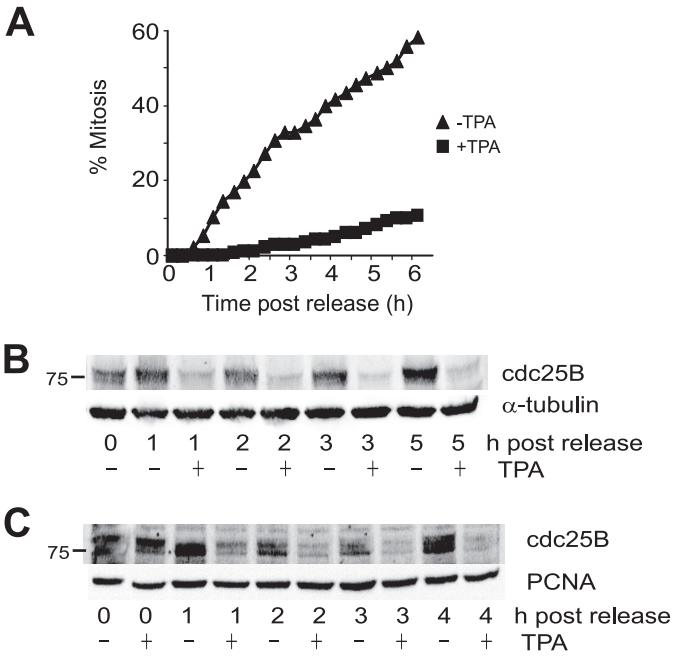

FIGURE 3. **MAPK signaling delays exit from G_2 phase checkpoint arrest.** *A*, etoposide-arrested G_2 phase HeLa cells were released into mitosis with caffeine either without (*triangles*) or with TPA addition (*squares*) followed by time lapse microscopy, and the cumulative mitotic index was assessed. *B*, lysates prepared from a parallel experiment to *A* were immunoblotted for cdc25B. α-Tubulin was a loading control. *C*, U2OS cells were arrested in G_2 phase using the topoisomerase II inhibitor ICRF193. Cells were then released from the checkpoint arrest with caffeine either with or without TPA addition. Cells were harvested at the indicated times after caffeine addition, and lysates were immunoblotted for cdc25B or PCNA as a loading control.

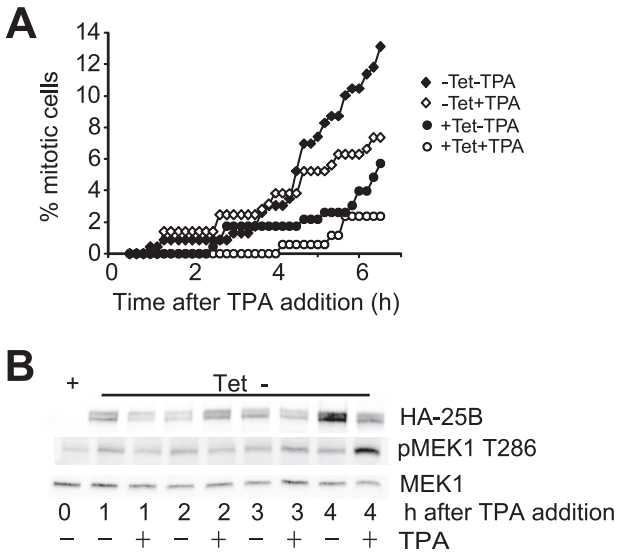

FIGURE 4. **Induced expression of cdc25B overcomes the MAPK signaling-induced G_2 phase delay.** *A*, U2OS cells expressing tetracycline (*Tet*)-repressed hemagglutinin (*HA*)-tagged cdc25B were arrested in G_2 phase using the topoisomerase II inhibitor ICRF193. Cells were then either maintained with tetracycline (*circles*) or derepressed by removal the tetracycline (*diamonds*) either with (*open symbols*) or without (*closed symbols*) TPA addition. Cells were then followed by time lapse microscopy, and the cumulative mitotic index was assessed. *B*, cells from an experiment similar to that shown in *A* were harvested at the indicated times after tetracycline removal, either with or without TPA addition. Cell lysates were immunoblotted for the exogenous HA-cdc25B (*HA-25B*), phospho-MEK1 Thr^{286} (*pMEK1 T286*) as a marker of entry into mitosis and MEK1 as a loading control.

the addition of the topoisomerase II poison etoposide (24). This suggested that activation of MAPK signaling would produce a robust delay in entry into mitosis. Because etoposide arrests cells with elevated levels of cdc25B (29), examination of the effect of TPA addition could provide further evidence for the loss of cdc25B being a consequence of destabilization of the protein. The checkpoint-arrested cells were driven into mitosis using caffeine to inhibit ATM/ATR. Strikingly, TPA addition effectively inhibited exit from checkpoint arrest and rapidly decreased the level of cdc25B protein (Fig. 3, *A* and *B*). The TPA-induced block of entry into mitosis and loss of cdc25B were strongly correlated and maintained for at least 5 h after TPA addition. This was also observed with TPA addition to U2OS cells arrested at the G_2 phase checkpoint using the topoisomerase II inhibitor ICRF193 and released from the arrest using caffeine (Fig. 3*C*).

The critical contribution of destabilizing cdc25B to the MAPK signaling-induced G_2 phase delay was demonstrated by the ability of exogenous cdc25B to overcome the delay. Inducible expression of cdc25B overcame the G_2 phase checkpoint arrest imposed by ICRF193 in U2OS cells, and addition of TPA had only a small effect on mitotic entry, correlated with TPA-induced destabilization of the exogenous cdc25B (Fig. 4, *A* and *B*). Similarly, transient overexpression of cdc25B promoted mitotic entry in TPA-treated, etoposide-arrested HeLa cells (supplemental Fig. S1). These data demonstrate that cdc25B levels are directly regulated by addition of TPA through regulation of cdc25B stability and that this destabilization of cdc25B underlies the G_2 delay observed with activation of MAPK in G_2 phase.

MAPK Signaling-induced G_2 Delay Is Independent of Known G_2 Checkpoint Pathways and p21^{CIP1} Induction—The mechanism by which EGF and TPA destabilized cdc25B to delay entry into mitosis was examined. The PKC inhibitor Gö6976 readily overcomes the G_2 phase delay induced by TPA addition (supplemental Fig. S2) and is also a potent inhibitor of the checkpoint signaling kinase Chk1, and possibly Chk2 (30), effectors of ATM/ATR checkpoint signaling. ATM and ATR cannot contribute to MAPK signaling-induced G_2 phase delay because it was imposed in the presence of caffeine, an inhibitor of ATM and ATR (Fig. 3*A*), and TPA did not increase the level of γH2Ax, or Chk1 or Chk2 phosphorylation, markers of DNA damage and ATM/ATR activity (31) (supplemental Fig. S3 and data not shown). To confirm that Chk1 and Chk2 were not involved in the MAPK-induced delay, Chk1 (Fig. 5*A*) and Chk2 (supplemental Fig. S4) were depleted using siRNA and shown to have no effect on the TPA-induced G_2 delay. We also failed to detect any increase in activation of p38MAPK with TPA addition, and the G_2 delay was insensitive to the p38MAPK inhibitor SB203580 (data not shown). Thus, the EGF/TPA-induced G_2 delay was independent of known checkpoint signaling mechanisms.

The contribution of MAPK signaling to the G_2 phase delay was initially investigated. TPA and EGF addition increased the phosphorylation of the activating Ser$^{218/222}$ residues on MEK1/2 (Fig. 5*B* and data not shown). Surprisingly, there was a small, but consistent decrease in ERK activation observed with TPA addition and little effect with EGF in G_2 phase cells

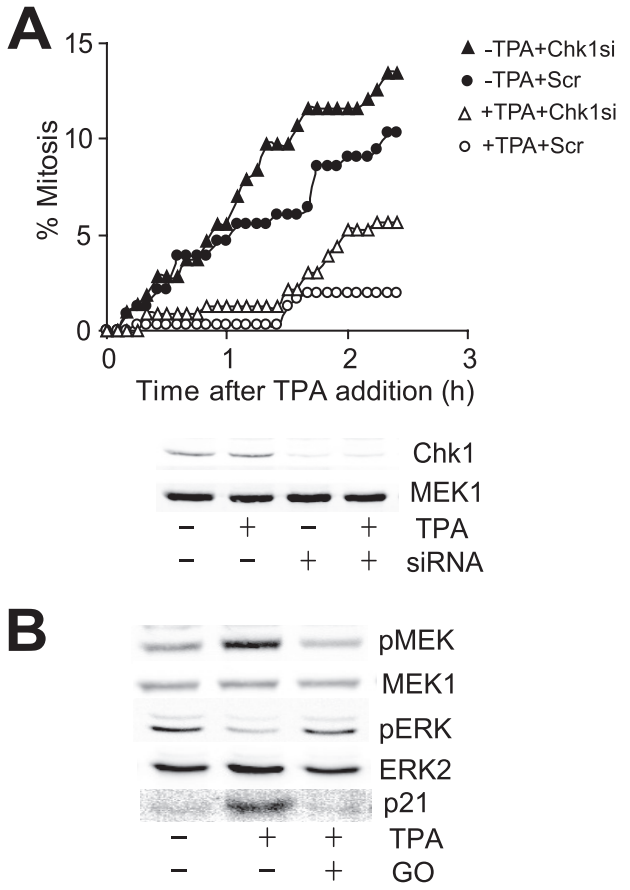

FIGURE 5. **MAPK signaling induced delay is independent of checkpoint signaling.** *A*, asynchronous HeLa cells were transfected with Chk1-directed (*triangles*) or scrambled (*Scr*) control (*circles*) siRNA for 24 h, treated with (*open symbols*) or without (*closed symbols*) TPA, then followed by time lapse microscopy; the cumulative mitotic indexed was then assessed. The degree of knockdown of each Chk1 is shown. MEK1 is a loading control. *B*, synchronized HeLa cells were treated with and without TPA and the PKC inhibitor Gö6976 in G_2 phase and then immunoblotted for the levels of phosphorylated $Ser^{218/222}$ MEK (*pMEK*), activated ERK (*pERK*), MEK1, ERK2, and p21 1 h later.

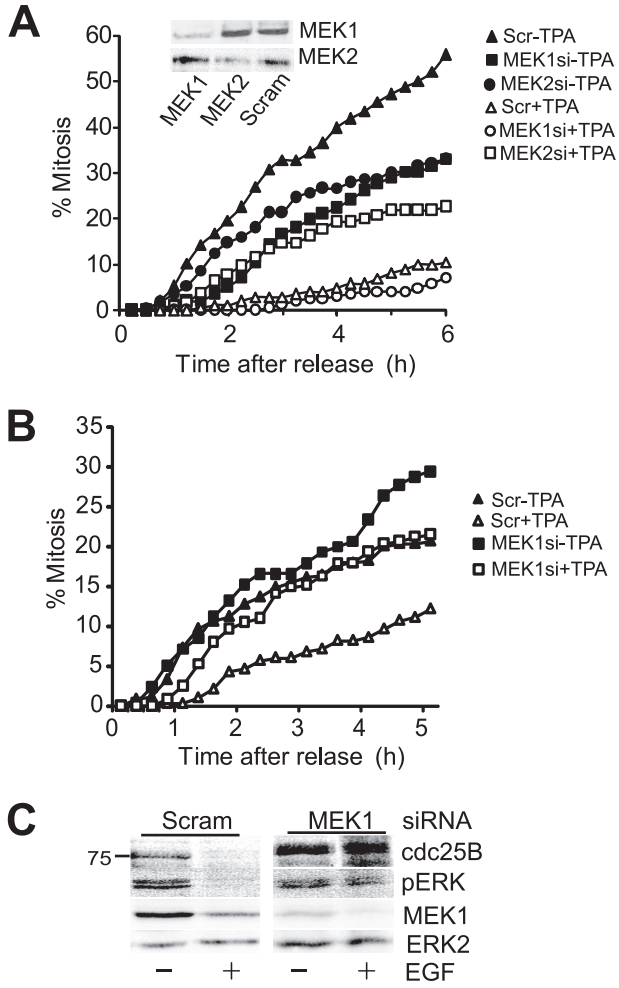

FIGURE 6. **G_2 delay depends on MEK1.** *A*, HeLa cells were initially transfected with either MEK1 (*squares*) or MEK2 (*circles*) directed or a scrambled (*Scr*) (*triangles*) siRNA, arrested in G_2 phase with etoposide, then released from the arrest by addition of caffeine, either with (*open symbols*) or without TPA (*closed symbols*). Cells were followed by time lapse microscopy and scored for entry to mitosis. *Inset*, the degree of MEK knockdown is shown. *B*, HeLa cells were treated with MEK1 (*squares*) or scrambled control (*triangles*) siRNA then arrested in G_2 phase etoposide as in *A*. Cells were released from the arrest with caffeine either without (*closed symbols*) or with addition of 100 ng/ml EGF (*open symbols*) and followed by time lapse microscopy as in *A*. *C*, cells from an experiment parallel to that shown in *B* were harvested 30 min after EGF treatment and immunoblotted for cdc25B, activated ERK (*pERK*), and MEK1. ERK2 was used as a loading control.

(Figs. 5*B* and 6*C*). There was a modest increase the cdk inhibitor $p21^{CIP1}$ that was blocked with the PKC inhibitor and previously demonstrated to be a downstream response to ERK activation (13), suggesting that there was a small increase that was masked by the level of activated ERK in G_2 phase cells. It was reported that an ERK-mediated increased $p21^{CIP1}$ expression was a major contributor to the TPA-induced G_2 delay (13, 32). To assess the role of $p21^{CIP1}$ in the G_2 delay directly, we reduced $p21^{CIP1}$ expression using siRNA. Knockdown of p21 using siRNA had no effect on the TPA-induced delay, demonstrating that $p21^{CIP1}$ expression did not contribute to the G_2 delay (supplemental Fig. S5). Treatment of cells with a histone deacetylase inhibitor induced a more robust expression of $p21^{CIP1}$ but only a minor delay in G_2/M progression (33), which was reduced by siRNA depletion, indicating that increased $p21^{CIP1}$ expression was not responsible for the TPA-induced G_2/M delay (supplemental Fig. 5).

MEK1 Is Specifically Required for the G_2 Delay following MAPK Pathway Activation—Whereas UO126 is a potent inhibitor of both MEK1 and MEK2, it also has other targets (34). To verify that U0126 inhibition of MEK was the basis for the partial rescue of delay, individual MEK isoforms were depleted using siRNA knockdown. Only siRNA knockdown of MEK1 rescued the TPA- and EGF-induced G_2 delay (Fig. 6, *A* and *B*) and rescued cdc25B stability (Fig. 6*C*).

To verify the MEK isoform-specific function, mouse embryonic fibroblasts (MEFs) generated from MEK1 and MEK2 knock-out mice, and knock-out MEFs reconstituted with the appropriate MEK (35, 36), were analyzed. TPA had no effect on mitotic entry in the MEK1 knock-out MEFs, but delayed entry into mitosis was observed in MEK1-reconstituted and MEK2 knock-out and reconstituted MEFs (Fig. 7). Thus, depletion of MEK1, but not MEK2, overcomes the G_2 delay and rescued the stability of cdc25B, showing that regulation of G_2/M progression by the MAPK module is mediated specifically through the MEK1 isoform. Taken together, these data suggest that regulation of cdc25B protein levels by

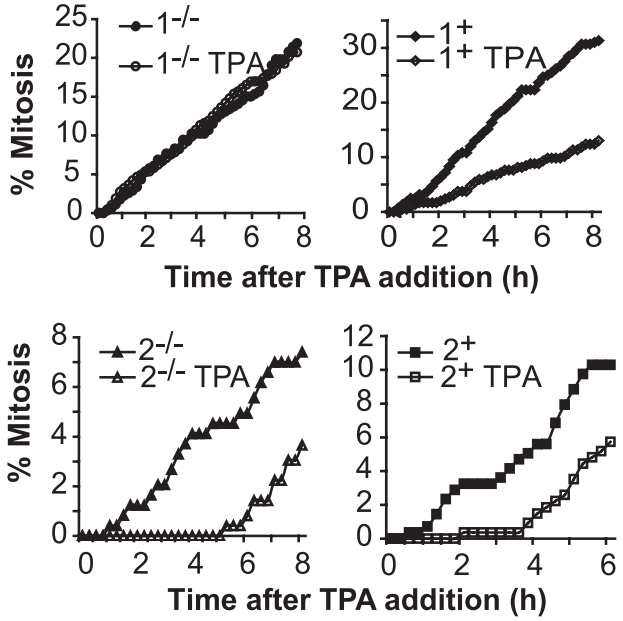

FIGURE 7. **G_2 delay depends on MEK1.** Asynchronous cultures of MEK1 knock-out (MEK1$^{-/-}$) and reconstituted (MEK1^{+}), and MEK2 knock-out (2$^{-/-}$) and knockouts reconstituted with MEK2 (2^{+}) MEFs were treated with TPA and followed by time lapse microscopy. The cumulative mitotic index was scored for each culture.

MEK1 functions as a direct link between the MAPK pathway and G_2/M cell cycle machinery.

Cdc25B Ser^{249} Is Phosphorylated in a MEK-dependent Manner and Destabilizes Cdc25B Protein—On SDS-PAGE, cdc25B runs as a broad band containing multiple discreet isoforms, which were reduced to a single band on treatment with λ-phosphatase, demonstrating that they represent phosphorylated forms of the protein (Fig. 8*A*). It was noted that when degradation of the destabilized cdc25B was blocked with the proteasome inhibitor MG132, the cdc25B band was retarded in its electrophoretic mobility (Figs. 2*A* and 8, *A* and *B*), which was also reduced to the same mobility band with phosphatase treatment *in vitro* (Fig. 8*A*). Addition of the MEK inhibitor U0126 effectively blocked the phosphorylation-dependent band shift in response to both TPA and EGF, indicating that this was a MEK-dependent phosphorylation (Fig. 8, *A* and *B*). Ser^{249} had previously been identified as a MK2 and p38MAPK phosphorylation site on cdc25B *in vitro* (37), and its proximity to the βTrCP-dependent DDG motif suggested that it may regulate that motif (38). HeLa cells expressing GFP-cdc25B showed a similar decreased mobility form on treatment with TPA, and this mobility change was blocked with mutation of Ser^{249} to Ala. Quantitation of the stability of the wild-type and S249A mutant showed that the mutant was more stable than the wild-type protein in both untreated and TPA-treated cells (Fig. 8*C*). Finally, an antibody specific for Ser(P)^{249} cdc25B detected this form of cdc25B in TPA-treated cells. This band ran above the 75 kDa marker, co-migrating with the slower migrating form of cdc25B. The Ser(P)^{249} band was increased with MG132 and completely lost with U0126 treatment (Fig. 8*D*). This demonstrates that the MEK-dependent destabilization of cdc25B was because of phosphorylation of Ser^{249} on cdc25B.

DISCUSSION

In this report we have demonstrated that activation of MAPK pathway signaling induces a G_2 phase delay via a MEK1-dependent mechanism culminating in the rapid destabilization of the critical G_2/M regulator cdc25B. Depletion and inhibition of cdc25B have previously been demonstrated to delay entry into mitosis (18, 39). Cdc25B cooperates with cdc25A in promoting normal G_2/M progression and hence induces only relatively short delay. However, cdc25B is specifically required for exit from a G_2 phase checkpoint arrest, and its depletion in this case causes a more significant delay in entry into mitosis (24). The relatively transient delay induced with EGF or TPA in normal cycling cells and more robust delay observed in the G_2 phase checkpoint-arrested cells driven into mitosis with caffeine exactly mirror the effects reported with siRNA-mediated depletion of cdc25B in these identical systems (18, 24). The lack of involvement of established pathways that promote a G_2 phase delay, ATM/ATR, Chk1/2, and p38MAPK checkpoint signaling is not surprising because these pathways impose a G_2 phase delay by regulating cdc25B activity (17, 21, 40, 41).

The contribution of upstream signaling through the MAPK pathway to the G_2 phase delay is demonstrated by the ability of both TPA and EGF to impose the delay, and the relatively short lived effect EGF compared with TPA reflects the relative duration of MAPK signaling generated by each stimulus. The discovery that MEK1 but not MEK2 depletion blocked the EGF- and TPA-induced destabilization of cdc25B and G_2 phase delay clearly demonstrates the involvement of MEK1 in this mechanism. In *Xenopus* extracts, MAPK activation causes a G_2 phase delay, attributed to ERK phosphorylation of Wee1, and phosphorylation of cdc25C by p90RSK, a downstream effector of ERK activity (42, 43). There is contradictory evidence of a role for MAPK signaling in G_2 and mitosis in mammalian cells (5, 6, 8), but recent evidence suggests that some of this maybe attributed to cell lineage-dependent differences (44). MAPK signaling has also been implicated in the G_2 arrest associated with overexpression of BRCA1 and p14ARF, although these mechanisms involved Chk1, differentiating them from the present study (45, 46).

The mechanism by which MEK1 destabilizes cdc25B appears to be through phosphorylation of Ser^{249}. Cdc25B stability is regulated in part by the Skp1/Cullin1/F-box E3 ubiquitin ligase β-TrCP, which recognizes a DDG motif in the N-terminal half of the protein (38). Interestingly, cdc25A, which is also regulated by β-TrCP, is the target for ERK-dependent phosphorylation, which accelerates its degradation in a manner similar to cdk1- and Chk1- dependent phosphorylation (47). The sensitivity of the Ser^{249} site to the MEK inhibitor U0126 and the fact that it was originally identified as a p38MAPK-dependent site implicate ERK as being responsible for the Ser^{249} phosphorylation. p38MAPK and ERK have similar phosphorylation site determinants with their *in vivo* specificity determined by specific docking site interactions (48). Additionally, TPA treatment rapidly inactivated p38MAPK, indicating that p38MAPK or MK2 was unlikely to be responsible for the phosphorylation observed (data not shown). Interestingly, Cdc25A destabilization in response to MAPK pathway activation was not detected

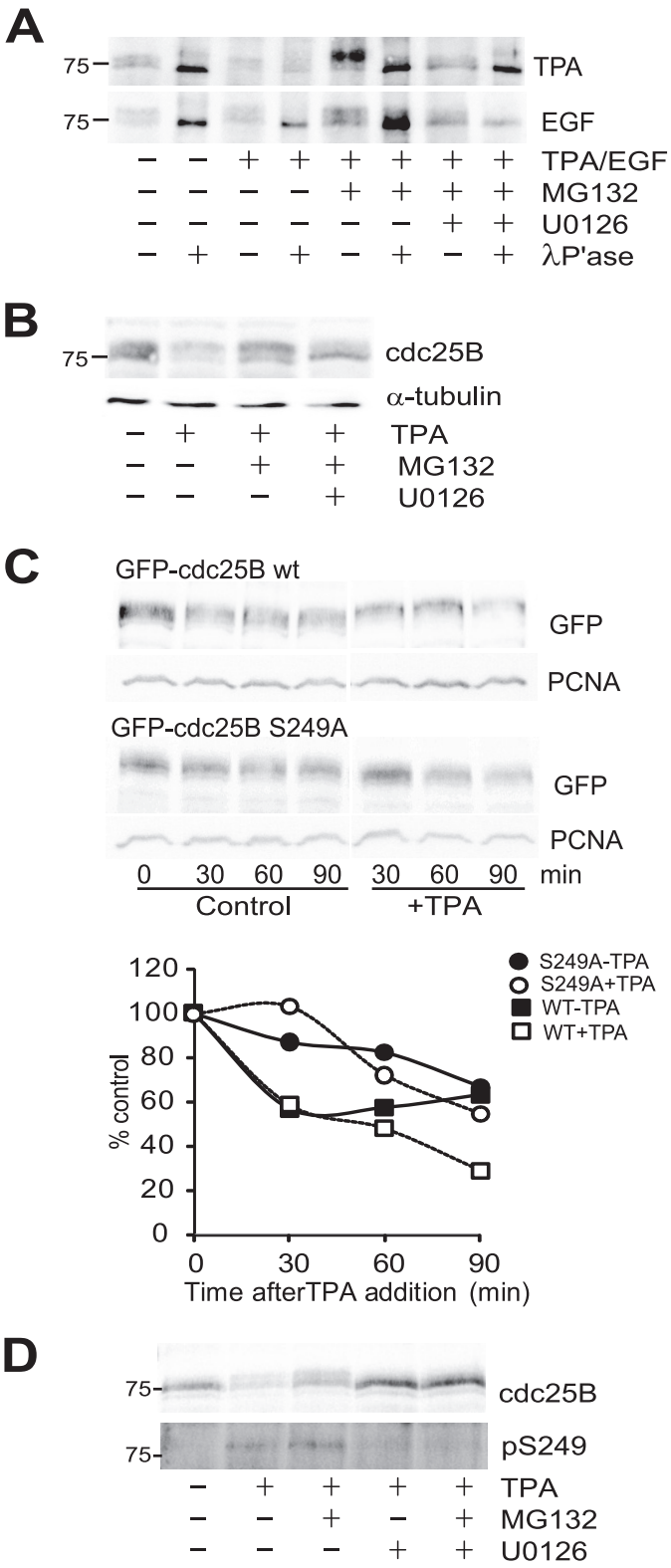

FIGURE 8. **MEK-dependent phosphorylation of Ser^{249} destabilizes cdc25B.** *A*, synchronized G_2 phase HeLa cells from either untreated control or 30 min after treatment with the indicated drugs, and either TPA (*upper panel*) or EGF (*lower panel*) was harvested and cdc25B immunoprecipitated. Half of each immunoprecipitate was treated with λ-phosphatase, then the immunoprecipitated protein was analyzed by immunoblotting for cdc25B. *B*, whole cell lysates from the TPA experiment shown in *A* were immunoblotted for cdc25B and α-tubulin as a loading control. *C*, HeLa cells were transfected with either GFP-cdc25B wild type (*WT*) or S249A mutant, then synchronized and treated with 10 μg/ml cycloheximide without (control) and with TPA. The quantitation of the level of cdc25B expressed as percent of zero time control is shown. The control data are the mean of three individual experiments. Wild type (*squares*) and S249A mutant cdc25B (*circles*) were treated without (*closed symbols*) or with (*open symbols*) TPA. *PCNA*, proliferating cell nuclear antigen. *D*, Cdc25B immunoprecipitated from synchronized G_2 phase HeLa cells 1 h after treatment with indicated drugs was immunoblotted for cdc25B or Ser(P)^{249} cdc25B. The position of the 75 kDa marker is shown.

in the current study. The reason for this is unclear. The inability of the MEK inhibitor U0126 to rescue the TPA/EGF-stimulated G_2 phase delay and cdc25B destabilization completely may point to mechanisms in addition to decreased stability of cdc25B being involved in the delay. The ability of MEK1 depletion to block the loss of cdc25B completely indicates that the effect is MEK1-dependent, with the Ser^{249} phosphorylation and resultant destabilization likely to depend on ERK activation. However, cdc25B is an unstable protein with a half-life of less than 30 min in G_2 phase cells (38). It is possible that in addition to the ERK-dependent Ser^{249} phosphorylation and destabilization of cdc25B, MEK1 also blocks *de novo* synthesis of cdc25B. This would also effectively deplete cdc25B levels and could act in cooperation with the destabilization of the preexisting pool of cdc25B to maintain the G_2 phase delay. The failure of the MEK inhibitor to rescue cdc25B levels completely suggests that the proposed block in *de novo* synthesis is independent of MEK1 catalytic activity.

Although there appears to be significant functional redundancy between MEK1 and MEK2, a MEK1-specific function has recently been reported. Knock-out of MEK1, but not MEK2, reduced tumor formation in a chemically induced mouse skin cancer model (49), suggesting a specific role for MEK1 in response to DNA-damaging agents. Our finding that the MEK1-dependent signaling, by targeting cdc25B stability, was capable of influencing the timing of exit from a G_2 phase DNA damage checkpoint arrest may contribute directly to this MEK1-specific effect on tumor formation.

The nature of the signal that stimulates the MEK1-dependent G_2 delay mechanism we have defined is at present unknown. We have demonstrated that it responds to external signals such as growth factors and other factors that stimulate MAPK signaling. Recently, hepatocyte growth factor used at physiological levels was shown to produce a similar G_2 phase delay (50). Other stresses affecting the cell microenvironment or its interactions with neighboring cells that generate MAPK-dependent signaling (51) would influence checkpoint exit though this MEK1-dependent mechanism. Thus, in response to stresses that produce both intracellular damage that triggers a G_2 phase checkpoint response through ATM/ATR signaling, and extracellular stress such as tissue damage triggering MAPK pathway activation, entry into mitosis would be delayed until both intracellular and extracellular stresses are resolved. This coordination between responses to intracellular and extracellular stress signals ensures that entry into mitosis only proceeds in optimal conditions to ensure the integrity of mitosis and proliferation of tissue following damage.

In conclusion, we have demonstrated that activation of MAPK signaling in G_2 phase cells induces a G_2 phase delay through a MEK1-dependent pathway. This pathway destabilizes cdc25B protein by increased phosphorylation of Ser^{249},

and it is the degradation of cdc25B that is responsible for the G_2 phase delay observed in normally cycling cells, and the sensitivity of cells attempting to exit a G_2 phase checkpoint arrest to MAPK signaling. Signaling through the MAPK pathway is critical for many biological activities, and upstream components of this pathway, notably Ras and Raf, are common targets for activating mutations in cancer. The demonstration that MEK1 can regulate normal G_2/M cell cycle and perhaps, more importantly, checkpoint mechanisms, suggests a novel mechanism by which these mutations can promote neoplastic transformation.

Acknowledgments—We thank Professor Bernard Ducommun for the Ser(P)^{249} antibody and inducible cdc25B U2OS cell line, and Professors John Whitehead and Roger Daly for critically reading of the manuscript.

REFERENCES

1. Harding, A., Tian, T., Westbury, E., Frische, E., and Hancock, J. F. (2005) *Curr. Biol.* **15,** 869–873
2. Widmann, C., Gibson, S., Jarpe, M. B., and Johnson, G. L. (1999) *Physiol. Rev.* **79,** 143–180
3. Edelmann, H. M., Kühne, C., Petritsch, C., and Ballou, L. M. (1996) *J. Biol. Chem.* **271,** 963–971
4. Lavoie, J. N., L'Allemain, G., Brunet, A., Müller, R., and Pouysségur, J. (1996) *J. Biol. Chem.* **271,** 20608–20616
5. Roberts, E. C., Shapiro, P. S., Nahreini, T. S., Pages, G., Pouyssegur, J., and Ahn, N. G. (2002) *Mol. Cell. Biol.* **22,** 7226–7241
6. Wright, J. H., Munar, E., Jameson, D. R., Andreassen, P. R., Margolis, R. L., Seger, R., and Krebs, E. G. (1999) *Proc. Natl. Acad. Sci. U.S.A.* **96,** 11335–11340
7. Liu, X., Yan, S., Zhou, T., Terada, Y., and Erikson, R. L. (2004) *Oncogene* **23,** 763–776
8. Shinohara, M., Mikhailov, A. V., Aguirre-Ghiso, J. A., and Rieder, C. L. (2006) *Mol. Biol. Cell* **17,** 5227–5240
9. Colanzi, A., Sutterlin, C., and Malhotra, V. (2003) *J. Cell Biol.* **161,** 27–32
10. El-Shemerly, M. Y., Besser, D., Nagasawa, M., and Nagamine, Y. (1997) *J. Biol. Chem.* **272,** 30599–30602
11. Barth, H., and Kinzel, V. (1994) *Exp. Cell Res.* **212,** 383–388
12. Barth, H., and Kinzel, V. (1995) *J. Cell. Physiol.* **162,** 44–51
13. Dangi, S., Chen, F. M., and Shapiro, P. (2006) *Cell Prolif.* **39,** 261–279
14. Klingler-Hoffmann, M., Barth, H., Richards, J., König, N., and Kinzel, V. (2005) *Eur. J. Cell Biol.* **84,** 719–732
15. O'Connell, M. J., Walworth, N. C., and Carr, A. M. (2000) *Trends Cell Biol.* **10,** 296–303
16. Bulavin, D. V., Amundson, S. A., and Fornace, A. J. (2002) *Curr. Opin. Genet. Dev.* **12,** 92–97
17. Manke, I. A., Nguyen, A., Lim, D., Stewart, M. Q., Elia, A. E., and Yaffe, M. B. (2005) *Mol. Cell* **17,** 37–48
18. Lindqvist, A., Källström, H., Lundgren, A., Barsoum, E., and Rosenthal, C. K. (2005) *J. Cell Biol.* **171,** 35–45
19. Gabrielli, B. G., De Souza, C. P., Tonks, I. D., Clark, J. M., Hayward, N. K., and Ellem, K. A. (1996) *J. Cell Sci.* **109,** 1081–1093
20. Xiao, Z., Chen, Z., Gunasekera, A. H., Sowin, T. J., Rosenberg, S. H., Fesik, S., and Zhang, H. (2003) *J. Biol. Chem.* **278,** 21767–21773
21. Uto, K., Inoue, D., Shimuta, K., Nakajo, N., and Sagata, N. (2004) *EMBO J.* **23,** 3386–3396
22. Boutros, R., Dozier, C., and Ducommun, B. (2006) *Curr. Opin. Cell Biol.* **18,** 185–191
23. Mailand, N., Falck, J., Lukas, C., Syljuâsen, R. G., Welcker, M., Bartek, J., and Lukas, J. (2000) *Science* **288,** 1425–1429
24. van Vugt, M. A., Brás, A., and Medema, R. H. (2004) *Mol. Cell* **15,** 799–811
25. Bansal, P., and Lazo, J. S. (2007) *Cancer Res.* **67,** 3356–3363
26. Theis-Febvre, N., Filhol, O., Froment, C., Cazales, M., Cochet, C., Monsarrat, B., Ducommun, B., and Baldin, V. (2003) *Oncogene* **22,** 220–232
27. Rossomando, A. J., Dent, P., Sturgill, T. W., and Marshak, D. R. (1994) *Mol. Cell. Biol.* **14,** 1594–1602
28. De Boer, L., Oakes, V., Beamish, H., Giles, N., Stevens, F., Somodevilla-Torres, M., Desouza, C., and Gabrielli, B. (2008) *Oncogene* **27,** 4261–4268
29. Gabrielli, B. G., Clark, J. M., McCormack, A. K., and Ellem, K. A. (1997) *Oncogene* **15,** 749–758
30. Kohn, E. A., Yoo, C. J., and Eastman, A. (2003) *Cancer Res.* **63,** 31–35
31. Jazayeri, A., Falck, J., Lukas, C., Bartek, J., Smith, G. C., Lukas, J., and Jackson, S. P. (2006) *Nat. Cell Biol.* **8,** 37–45
32. Barboule, N., Lafon, C., Chadebech, P., Vidal, S., and Valette, A. (1999) *FEBS Lett.* **444,** 32–37
33. Qiu, L., Burgess, A., Fairlie, D. P., Leonard, H., Parsons, P. G., and Gabrielli, B. G. (2000) *Mol. Biol. Cell* **11,** 2069–2083
34. Davies, S. P., Reddy, H., Caivano, M., and Cohen, P. (2000) *Biochem. J.* **351,** 95–105
35. Giroux, S., Tremblay, M., Bernard, D., Cardin-Girard, J. F., Aubry, S., Larouche, L., Rousseau, S., Huot, J., Landry, J., Jeannotte, L., and Charron, J. (1999) *Curr. Biol.* **9,** 369–372
36. Bélanger, L. F., Roy, S., Tremblay, M., Brott, B., Steff, A. M., Mourad, W., Hugo, P., Erikson, R., and Charron, J. (2003) *Mol. Cell. Biol.* **23,** 4778–4787
37. Lemaire, M., Froment, C., Boutros, R., Mondesert, O., Nebreda, A. R., Monsarrat, B., and Ducommun, B. (2006) *Cell Cycle* **5,** 1649–1653
38. Kanemori, Y., Uto, K., and Sagata, N. (2005) *Proc. Natl. Acad. Sci. U.S.A.* **102,** 6279–6284
39. Goldstone, S., Pavey, S., Forrest, A., Sinnamon, J., and Gabrielli, B. (2001) *Oncogene* **20,** 921–932
40. Schmitt, E., Boutros, R., Froment, C., Monsarrat, B., Ducommun, B., and Dozier, C. (2006) *J. Cell Sci.* **119,** 4269–4275
41. Boutros, R., Lobjois, V., and Ducommun, B. (2007) *Nat. Rev. Cancer* **7,** 495–507
42. Walter, S. A., Guadagno, S. N., and Ferrell, J. E., Jr. (2000) *Mol. Biol. Cell* **11,** 887–896
43. Chun, J., Chau, A. S., Maingat, F. G., Edmonds, S. D., Ostergaard, H. L., and Shibuya, E. K. (2005) *Cell Cycle* **4,** 148–154
44. Dumesic, P. A., Scholl, F. A., Barragan, D. I., and Khavari, P. A. (2009) *J. Cell Biol.* **185,** 409–422
45. Yan, Y., Spieker, R. S., Kim, M., Stoeger, S. M., and Cowan, K. H. (2005) *Oncogene* **24,** 3285–3296
46. Eymin, B., Claverie, P., Salon, C., Brambilla, C., Brambilla, E., and Gazzeri, S. (2006) *Cell Cycle* **5,** 759–765
47. Isoda, M., Kanemori, Y., Nakajo, N., Uchida, S., Yamashita, K., Ueno, H., and Sagata, N. (2009) *Mol. Biol. Cell* **20,** 2186–2195
48. Mayor, F., Jr., Jurado-Pueyo, M., Campos, P. M., and Murga, C. (2007) *Cell Cycle* **6,** 528–533
49. Scholl, F. A., Dumesic, P. A., Barragan, D. I., Harada, K., Charron, J., and Khavari, P. A. (2009) *Cancer Res.* **69,** 3772–3778
50. Nam, H. J., Kim, S., Lee, M. W., Lee, B. S., Hara, T., Saya, H., Cho, H., and Lee, J. H. (2008) *Cell. Signal.* **20,** 1349–1358
51. McKay, M. M., and Morrison, D. K. (2007) *Oncogene* **26,** 3113–3121